IEEE Access
Multidisciplinary | Rapid Review | Open Access Journal

Received September 3, 2019, accepted October 16, 2019, date of publication October 28, 2019, date of current version November 13, 2019.

Digital Object Identifier 10.1109/ACCESS.2019.2949842

Removal of ECG Artifacts From EEG Using an Effective Recursive Least Square Notch Filter

CHENXI DAI, JIANJIE WANG, JIALING XIE, WEIMING LI, YUSHUN GONG, AND YONGQIN LI, (Member, IEEE)

Department of Biomedical Engineering and Imaging Medicine, Army Medical University, Chongqing 400038, China

Corresponding author: Yongqin Li (leeoken@aliyun.com)

This work was supported by the National Nature Science Foundation of China under Grant 31771070.

ABSTRACT Electroencephalogram (EEG) is a common tool for medical diagnosis, cognitive research, and managing neurological disorders. However, EEG is usually contaminated with various artifacts, making it difficult to interpret EEG data. In this study, a recursive least square (RLS) notch filter was developed to effectively suppress electrocardiogram (ECG) artifacts from EEG recordings. ECG artifacts were estimated and modeled using the instantaneous frequency of the cardiac cycle. Then it was adaptively estimated using a RLS filter and directly subtracted from contaminated EEG data. Based on the validation measures of improvement of normalized power spectrum (INPS), mean square error (MSE) and information quantity (IQ), the performance of ECG artifacts suppression was compared among the proposed RLS approach, independent component analysis (ICA) and blind deconvolution method under information maximization (Infomax) on simulated and animal experimental data. Simulation data demonstrated that INPS of RLS method (19.75(18.37,20.95) dB) was significantly higher than that of ICA (4.35(3.35,5.41) dB) and Infomax (5.76(4.60,6.88) dB). Meanwhile, MSE of RLS method (0.20(0.08,0.53) μV^2) was considerably lower than that of ICA (5.59(2.35,19.79) μV^2) and Infomax (3.21(1.01,10.69) μV^2). Animal experimental data showed that INPS was 1.76(0.42,9.40) dB for RLS method, which was dramatically higher than that of ICA (0.02(0.00,0.14) dB) and Infomax (0.57(0.08,2.45) dB). The calculated IQ for RLS method (0.331(0.021,0.584)) was relatively lower than that of raw EEG (0.350(0.070,0.586)), ICA (0.350(0.069,0.581)) and Infomax (0.341(0.050,0.585)). The RLS notch filter can effectively eliminate ECG artifacts from EEG and preserve the majority of EEG information with little loss.

INDEX TERMS ECG artifacts, EEG, notch filter, recursive least square.

I. INTRODUCTION

Electroencephalogram (EEG) is an electrophysiological monitoring tool to record brain activity with the characteristics of convenient acquisition, noninvasive access, and high temporal resolution [1]. Quantitative EEG is a common method for medical diagnosis, cognitive research, and managing neurological disorders. In practical applications, EEG can be very easily contaminated by various artifacts due to its small amplitude and randomness. Interfering signals from technical or physiological sources firstly make the analysis and interpretation of EEG signals difficult, then corrupt the quantitative EEG results, and eventually affect the diagnosis of cortical activity [2].

Technical interference often contains bad contact of electrode, power induction, or electromagnetic interference, which can be readily solved during recording. Physiological interference is often caused by ocular movements, eye blinks, muscle artifacts, or cardiac electrical fields from the heart beat [3]. Electrocardiogram (ECG) artifacts, even below the visible level, have been shown to significantly degrade the quality of quantitative EEG measures [4], [5]. Furthermore, cardiac interference recorded by EEG electrodes often presents spiky, quasi-periodic signals, which can seriously affect EEG basic rhythm waves (0-30Hz) [6]. Hence, it is a huge challenge to analyze and interpret brain activity under ECG artifacts in practices.

The associate editor coordinating the review of this manuscript and approving it for publication was Kemal Polat.

To remove ECG artifacts, numerous methods have been developed. Traditional filters work well to eliminate electrical line noise and other high-frequency artifacts, but they can result in the loss of EEG components because ECG artifacts have a spectral overlap with underlying EEG signals [7], [8]. For the cardiac artifact correction methods in the time domain, such as Wiener filter and adaptive filter, the ECG artifacts may be overestimated and some useful EEG information may be lost after rejection because there is a cross-interference between ECG and EEG and these two kinds of signals can be influenced by each other [9]. Independent component analysis (ICA) was also used to eliminate the ECG artifacts from EEG waveform by researchers [2], [8], [10]. Devuyst et al. proposed a modified blind deconvolution approach based on information maximization (Infomax) theory in cancelling cardiac artifacts from single-channel EEG, but its filter length and filter coefficient are required to be estimated for each segment [11]. However, some limitations still need to be improved for above methods. Firstly, those methods were found to be inefficient and the artifacts were still visible after removing ECG interference since the real cardiac interference exhibit remarkably different waveforms compared to ECG, which may be difficult for deconvolution or adaptive filtering methods [12]. Secondly, many EEG channels were required for those methods to better remove cardiac interference and their performance may not work very well for single EEG channel situation. Lastly, some methods suggest that EEG signal should be split into various short segments, and for each segment, specific parameters, such as the filter length and weight coefficients, need to be determined repeatedly before removing artifacts, which is very time consuming and tedious [11].

In this paper, a recursive least square (RLS) algorithm, which is derived from a modification of the notch filter based on the least mean squares (LMS) method, was proposed. The RLS algorithm can effectively suppress cardiac interference only using a single-channel EEG and ECG, and does not need to estimate any parameters. In order to verify its effectiveness in terms of the performance of ECG artifacts suppression and preservation of underlying EEG rhythms, including the improvement of normalized power spectrum (INPS), mean square error (MSE) and information quantity (IQ), other two established methods, ICA and Infomax methods, were implemented and compared to the new algorithm on simulated and animal experimental data.

II. MATERIALS AND METHODS

As a classic adaptive filter, LMS algorithm has been widely employed to remove various artifacts including ocular movements, eye blinks, muscle artifacts, from EEG [13]–[15]. Figure 1 shows an example of ECG and EEG simultaneously recorded on rat 3 min after induction of asphyxial cardiac arrest. In this phase, no underlying EEG rhythm should be observed since EEG became isoelectric after 1 min of cardiac arrest [16], [17]. However, the recorded EEG waveform did not show as a flat trace and clearly ECG artifacts

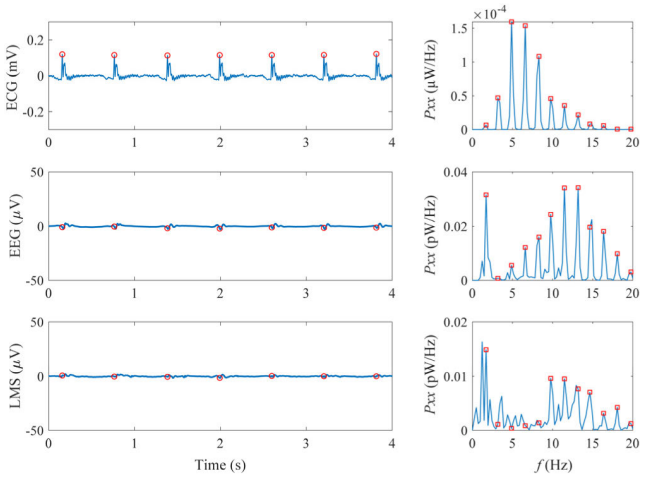

FIGURE 1. An illustration of ECG and EEG corrupted by ECG artifacts simultaneously recorded on a rat during asphyxial cardiac arrest. Left panels are time domain and right panels are frequency domain. The power spectral density (P_{xx}) is calculated using the Welch method and 4-s rectangular window. Red circles in ECG recording represent R peaks. Red square markers shown in the frequency domain represent ECG harmonics. LMS, least mean squares.

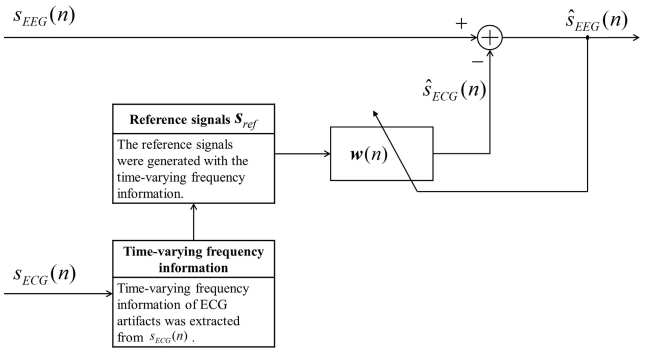

FIGURE 2. Diagram of the RLS notch filter for ECG artifacts suppression. $s_{EEG}(n)$ and $s_{ECG}(n)$ are corrupted EEG signal and ECG signal, respectively. The reference signals $s_{ref}(n)$ are computed using the time-varying frequency information extracted from ECG. An estimate of the artifacts, $\hat{s}_{ECG}(n)$, is subtracted from $s_{EEG}(n)$ to obtain the clean EEG $\hat{s}_{EEG}(n)$. The filter coefficients $w(n)$ are updated using the RLS method.

were observed. In the time domain, the highly correlated consistency and synchronization between QRS complexes and EEG spikes demonstrated that artifacts in EEG waveform were generated by cardiac activity. After denoising with the LMS, although the interference was greatly suppressed, the residual artifact appeared in the filtered EEG waveform may still lead to improper interpretation. Further analysis in the frequency domain revealed that artifacts are mainly composed of harmonics with the fundamental frequency of beat to beat. Based on above observation and previous reports [18], we modeled ECG artifacts as a harmonic signal and modified the LMS algorithm using the frequency of the instantaneous beat to beat rate as the fundamental frequency.

A. RLS NOTCH FILTER

The structure of the RLS notch filter was depicted in Figure 2. The implementation of the method consists of the following five steps.

Step one: time-varying frequency information of cardiac artifacts was extracted from the ECG signal. It is hypothesized that the ECG artifacts can be modeled as an almost periodic signal, with the fundamental frequency of the adjacent R peaks in ECG signal. The instantaneous frequency f_i and phase $\phi(n)$ of the ECG artifacts can be obtained by using a given series of successive R peaks n_i ($i = 1, 2, \cdots m$) in ECG waveform and a sampling rate Fs [19],

$$f_i = \begin{cases} \dfrac{Fs}{n_2 - n_1}, & n \le n_1, \\ \dfrac{Fs}{n_{i+1} - n_i}, & n_i < n \le n_{i+1},\ i = 1, 2, \cdots m-1, \\ \dfrac{Fs}{n_m - n_{m-1}}, & n > n_m, \end{cases} \quad (1)$$

and

$$\phi(n) = \begin{cases} \dfrac{2\pi(n - n_1)}{n_2 - n_1}, & n \le n_1, \\ \dfrac{2\pi(n - n_i)}{n_{i+1} - n_i}, & n_i < n \le n_{i+1},\ i = 1, 2, \cdots m-1, \\ \dfrac{2\pi(n - n_m)}{n_m - n_{m-1}}, & n > n_m, \end{cases} \quad (2)$$

where m represents the total number of R peaks. To supplement the frequency information before the first and after the last R peaks, two smooth transition periods were defined. The first transition period was defined as the duration from the beginning of recording to the first R peak and its frequency information was identical to the first cardiac cycle (refer to the first formula in (1) and (2)). The second transition period was defined as the duration from the last R peak to the ending of recording and its frequency information was identical to the last cardiac cycle (refer to the last formula in (1) and (2)). The above procedure estimated the time-varying frequency information of the ECG artifacts using the marker events method [19] and the R peaks in ECG was taken as markers. The interval between consecutive marks corresponds to one cardiac cycle. It was assumed that during a cardiac cycle, the frequency of ECG artifacts is constant, but that it may vary between cycles. For each segment, a reliable QRS detection algorithm was used to locate the R peaks in the ECG [20]. Then subsequent manual inspection and correction were implemented to ensure accurate location of R peaks. If inaccurate time varying frequency information was obtained in this step, ECG artifacts would be overestimated or underestimated and then EEG quality could be decreased. Thus, the acquisition of time varying frequency information of ECG is an important and indispensable step throughout the filtering process.

Step two: the reference signals $\boldsymbol{s}_{ref}(n)$ were generated with the time-varying frequency information. The reference signals $\boldsymbol{s}_{ref}(n)$ for N harmonics are expressed as a column vector,

$$\begin{aligned} \boldsymbol{s}_{ref}(n) &= \begin{bmatrix} \boldsymbol{s}_I(n) \\ \boldsymbol{s}_Q(n) \end{bmatrix}, \\ \boldsymbol{s}_I(n) &= [\cos(\phi(n)), \cos(2\phi(n)), \cdots, \cos(N\phi(n))]^T, \\ \boldsymbol{s}_Q(n) &= [\sin(\phi(n)), \sin(2\phi(n)), \cdots, \sin(N\phi(n))]^T, \end{aligned} \quad (3)$$

where N is the number of harmonics considered in cardiac artifacts, $(.)^T$ denotes the vector/matrix transpose, $\boldsymbol{s}_I(n)$ donates in-phase part and $\boldsymbol{s}_Q(n)$ donates quadrature part, according to that any signal can be represented by the in-phase and quadrature decomposition of the sinusoidal interference of known frequency [21].

Step three: the model of time-varying ECG artifacts was constructed by using the generated reference signals. The ECG artifacts model $\hat{s}_{ECG}$ was expressed as

$$\begin{aligned} \hat{s}_{ECG}(n) &= \boldsymbol{w}(n)^T \boldsymbol{s}_{ref}(n) \\ &= \boldsymbol{a}(n)^T \boldsymbol{s}_I(n) + \boldsymbol{b}(n)^T \boldsymbol{s}_Q(n) \\ &= \sum_{k=1}^{N} a_k(n)\cos(k\phi(n)) + b_k(n)\sin(k\phi(n)), \\ \boldsymbol{w}(n) &= \begin{bmatrix} \boldsymbol{a}(n) \\ \boldsymbol{b}(n) \end{bmatrix}, \\ \boldsymbol{a}(n) &= [a_1(n), a_2(n), \cdots, a_N(n)]^T, \\ \boldsymbol{b}(n) &= [b_1(n), b_2(n), \cdots, b_N(n)]^T, \end{aligned} \quad (4)$$

where the filter coefficients $\boldsymbol{w}(n)$ at time n include two parts, in-phase coefficients $\boldsymbol{a}(n)$ and quadrature coefficients $\boldsymbol{b}(n)$. $\boldsymbol{a}(n)$ is the coefficients for the in-phase decomposition of reference signals $\boldsymbol{s}_I(n)$ and $\boldsymbol{b}(n)$ is the coefficients for the quadrature decomposition of reference signals $\boldsymbol{s}_Q(n)$. During the R-R intervals, the model of ECG artifacts can be expressed through its Fourier series representation in trigonometric form using harmonics of time-varying in-phase coefficients $\boldsymbol{a}(n)$ and quadrature coefficients $\boldsymbol{b}(n)$. These coefficients' values change slowly in time and serve to track the changes in waveform from cycle to cycle. The fundamental frequency also changes between adjacent cardiac cycles (refer to (1) and (2)).

Step four: the clean EEG was obtained by subtracting the estimation of ECG artifacts from input EEG signal. The clean EEG was then computed as

$$\hat{s}_{EEG}(n) = s_{EEG}(n) - \hat{s}_{ECG}(n), \quad (5)$$

where $s_{EEG}(n)$ is the EEG signal corrupted by ECG artifacts.

Step five: the RLS method was employed to update the filter coefficients $\boldsymbol{w}(n)$. The criterion is to minimize an exponentially weighted cost function

$$\begin{aligned} J(n) &= \sum_{i=0}^{n} \lambda^{n-i} \left| s_{EEG}(i) - \hat{s}_{ECG}(n) \right|^2 \\ &= \sum_{i=0}^{n} \lambda^{n-i} \left| s_{EEG}(i) - \boldsymbol{w}(n)\boldsymbol{s}_{ref}(i) \right|^2, \end{aligned} \quad (6)$$

where λ denotes forgetting factor. The solution of the RLS algorithm is determined as [22]

$$\begin{aligned} \boldsymbol{w}(n) &= \boldsymbol{R}^{-1}(n)\boldsymbol{r}(n), \\ \boldsymbol{R}(n) &= \sum_{i=0}^{n} \lambda^{n-i} \boldsymbol{s}_{ref}(i)\boldsymbol{s}_{ref}(i)^T, \\ \boldsymbol{r}(n) &= \sum_{i=0}^{n} \lambda^{n-i} \boldsymbol{s}_{ref}(i) s_{EEG}(i) \end{aligned} \quad (7)$$

where $\boldsymbol{R}(n)$ and $\boldsymbol{r}(n)$ represent the autocorrelation and mutual correlation matrix respectively. To facilitate iterative update of $\boldsymbol{w}(n)$, the RLS algorithm is formulated and implemented in this way [23]

$$\begin{aligned} \boldsymbol{k}(n) &= \frac{\boldsymbol{R}^{-1}(n-1)\boldsymbol{s}_{ref}(n)}{\lambda + \boldsymbol{s}_{ref}(n)^T\boldsymbol{R}^{-1}(n-1)\boldsymbol{s}_{ref}(n)}, \\ \boldsymbol{R}^{-1}(n) &= \frac{1}{\lambda}\left[\boldsymbol{R}^{-1}(n-1) - \boldsymbol{k}(n)\boldsymbol{s}_{ref}(n)^T\boldsymbol{R}^{-1}(n-1)\right], \\ \boldsymbol{w}(n) &= \boldsymbol{w}(n-1) + \boldsymbol{k}(n)\hat{s}_{EEG}(n), \end{aligned} \tag{8}$$

where $\boldsymbol{R}^{-1}(n)$ is the inverse of $\boldsymbol{R}(n)$. The time-varying coefficients $\boldsymbol{w}(n)$ of the artifacts model are usually estimated through an adaptive filter that tracks the evolution of the spectral composition of the ECG artifacts, which are often updated using the LMS method [21], [24], [25]. The RLS method is employed to update $\boldsymbol{w}(n)$ with a view of its faster convergence rates and less sensitivity to variations compared to the LMS method [26]. Note that $N = 25$ and $\boldsymbol{R}(0) = \delta\boldsymbol{I}$, where δ is a small initial constant and set $\delta = 0.0001$ in this study, and $\boldsymbol{I}$ is an identity matrix.

B. SIMULATED DATA

To obtain optimal parameters' value and validate the performance of RLS notch filter with known clean EEG signal and artifact, a simulated data was generated. The simple periodic signal $s(t)$ was used to simulate burst suppression rhythm, which denotes the clean EEG signal. The ECG extracts were acquired from 9 healthy Sprague–Dawley rats (323.7±34.4 g). A 10-oreder filter was used to convert ECG signals to cardiac interference and the coefficients of its impulse response were randomly generated at each creation of an artificial signal $e(t)$ [27].

As a result, the artifact-contaminated EEG signals can be generated by clean EEG signal $s(t)$ with the ECG interference signal $e(t)$ in the following manner:

$$\begin{aligned} x(t) &= s(t) + c \cdot e(t), \\ s(t) &= \sin(2\pi t + 0.1\pi) + \sin(6\pi t + 0.2\pi) \\ &\quad + \sin(10\pi t + 0.3\pi) + \sin(15\pi t + 0.4\pi) \\ &\quad + \sin(20\pi t + 0.5\pi), \end{aligned} \tag{9}$$

where $x(t)$ is the synthetic EEG signal corrupted by ECG artifacts, and c is a scale coefficient. By changing the value of c, EEG and ECG artifacts were mixed together in the case of different signal to noise ratio (SNR) levels with −15dB, −10dB, −5dB, and 0dB. For each SNR, 135 4-s artifact-contaminated EEG segments (15 segments in each animal) were generated. Sampling rate was 1000 Hz.

Performance of RLS notch filter was investigated for increasing the forgetting factor λ ($\lambda = 0, 0.05, \cdots, 1$). Furthermore, we also compared the performance of other two different single-channel methods, ICA approach (FastICA) [8] and blind source separation approach based on information maximization (Infomax) [11], using their optimal parameters.

C. ANIMAL EXPERIMENTAL DATA

In order to further verify the performance of the proposed method in experimental data with unknown clean signal and artifact, EEG and ECG signals were recorded from rats resuscitated after 7-min untreated asphyxial cardiac arrest and cardiopulmonary resuscitation [16]. Specifically, EEG data were recorded with a differential preamplifier (PRE-ISO.EEG100, Xiangyun Computing Technology, Beijing, China) from two bipolar channels (C3–P3, C4–P4 according to the 10–20 system). Four subcutaneous needle electrodes were placed at central and parietal skull positions on each side, in addition to one combined electrode functioning as reference and ground. The amplifier gain of each channel was set at 10,000, and the cutoff frequencies were set at 0.3 and 70 Hz for the high-pass and low-pass filters, respectively. EEG and ECG were synchronously recorded through a data acquisition system supported by Windaq hardware/software (Dataq Instruments Inc., Akron, OH, USA) at a sample rate of 1000 Hz respectively.

The EEG rhythms are usually annotated and classified as one of the three following categories: isoelectric/suppression, burst suppression, and continuous background EEG activity [17], [28]. Isoelectric/suppression was defined as there is not any visible EEG activity (maximum voltage $< 5\ \mu$V) during a 30-s recording episode. Burst suppression was defined by the presence of clear increases in amplitude (burst, amplitude $>10\ \mu$V) followed by interburst intervals of at least 0.5 s without EEG activity or low amplitude activity (suppression, $<10\ \mu$V).

340 isoelectric, 374 burst suppression and 255 continuous background EEG 4-s segments contaminated by ECG artifacts were cut off from rats. Since identical waveforms was observed between the two EEG channels during the animal experiment, the C3-P3 channel of each segment with obvious ECG artifacts was employed to perform ECG artifacts rejection by using the proposed method.

D. QUANTITATIVE VALIDATION MEASURES

In order to evaluate the performance of the ECG artifacts removal methods, three indicators, INPS [8], MSE, and IQ [29] were used in our study. INPS was employed to evaluate the results of ECG artifacts suppression on simulated and real data. Because both background EEG activity and ECG artifacts were unknown in EEG signals from animal experimental data, MSE cannot be taken as the quantitative validation criteria of artifact rejection. Thus, MSE was used for evaluating the preservation of EEG information on simulated and IQ was taken as the quantitative validation criteria for EEG information preservation on animal data.

EEG power improvement in frequency windows of 0.5 Hz centered at the peaks of the ECG harmonics was used as an estimator, INPS [8]. The normalized power spectral density of 4-s recordings was first calculated, after passing data through rectangular window, using the Welch method. Within each window the power was calculated before and after ECG

artifacts removal. INPS is expressed as a ratio of sums of the windowed power of EEG by the formula:

$$INPS = 10\log_{10}\frac{\sum_{f_I} P_{s_{EEG}}(f_I)}{\sum_{f_I} P_{\hat{s}_{EEG}}(f_I)},$$
$$f_I \in \{f \,||f - kf_0| < 0.5\text{Hz}\,, k = 1, 2, \cdots, N\}, \quad (10)$$

where N is the number of harmonics, and f_0 is the mean fundamental frequency of ECG signal in the time window. INPS can indicate whether ECG-related interference, including its harmonics, was effectively suppressed. The higher the value of INPS is, the higher performance of ECG artifacts removal methods is. Thus, the INPS can be employed to evaluate the results of ECG artifacts suppression.

The value of MSE indicates the degree of similarity between two signals. The MSE of signals can be calculated by

$$MSE = \frac{1}{n}\sum_{i=1}^{n}(x_i - y_i)^2, \quad (11)$$

where x_i represents clean EEG signal, y_i denotes EEG signal after removing ECG artifacts, and n is the total time points of samples. The smaller the value of MSE is, the higher the similarity degree between two signals is. Thus, the MSE can be used to measure the degree of EEG information reservation after removing ECG artifacts.

An established quantitative EEG assessment method named IQ was used to analyze EEG signal before and after denoising and the detailed calculation procedure was described in [29]. Higher IQ corresponds to greater randomness measured by the entropy of the EEG rhythm. The lower the value of IQ is, the lower components of ECG artifacts in remained signal are. Thus, the IQ can be used to measure the degree of EEG information reservation after removing ECG artifacts. Usually, the value of isoelectric EEG ranges from 0 to 0.1, the value of burst suppression EEG ranges from 0.1 to 0.6, and the value of continuous background EEG is often larger than 0.6 [16], [29].

E. STATISTICAL ANALYSIS

Statistical analysis was performed with SPSS 19.0 software (SPSS, Chicago, IL, USA). Since data of INPS, MSE and IQ do not obey normal distribution, their median with the corresponding first and third quartiles (Q1-Q3) was reported and Friedman's analysis of variance (ANOVA) with its post hoc test was used to analyze the difference among all methods. $P<0.05$ was considered statistically significant.

III. RESULTS

A. REMOVING ECG ARTIFACTS FROM SIMULATED EEG SIGNALS

In the simulation study, relationships between INPS/MSE and forgetting factor after removing ECG artifacts using the RLS method at a SNR of −15 dB, −10 dB, −5 dB, 0 dB were firstly investigated. As shown in Figure 3, INPS has the lowest value and MSE has the highest value when the forgetting factor is equal to 0. But when forgetting factor is greater than 0.05, increasing its value will not influence INPS and MSE at each SNR level. According to the above simulation results, because the performance of RLS notch filter did not largely depend on the change of forgetting factor, a value of 0.5 was chose for the forgetting factor in the following calculation.

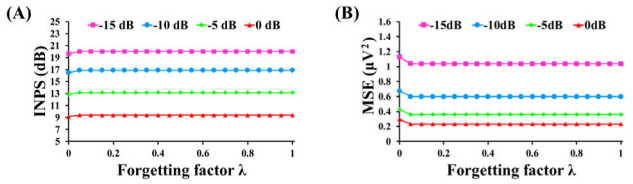

FIGURE 3. An illustration of the tendency of INPS and MSE under different forgetting factor λ and SNRs for RLS method. (A) INPS (B) MSE. INPS, improvement of normalized power spectrum. MSE, mean square error. SNR, signal to noise ratio. RLS, recursive least squares.

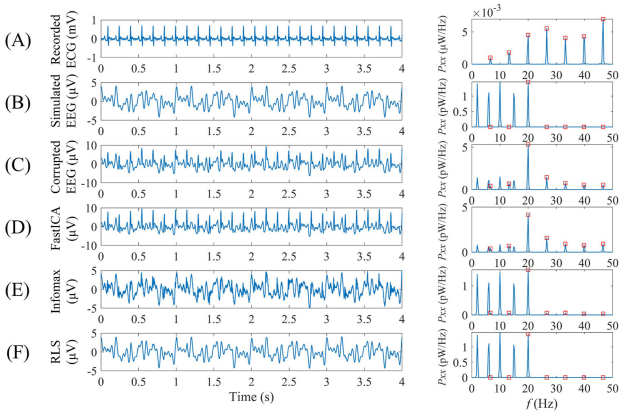

FIGURE 4. An example of simulated EEG signal before and after removing ECG artifacts in time and frequency domain. (A) ECG recorded from rat (B) simulated EEG (C) corrupted EEG (D) FastICA (E) Infomax (F) RLS. The power spectral density (P_{xx}) is calculated using the Welch method and 4-s rectangular window. Red square markers shown in the frequency domain represent ECG harmonics. ICA, independent component analysis. Infomax, information maximization. RLS, recursive least squares.

An example for artifact-contaminated simulated EEG signal before and after removing ECG artifacts in the time and frequency domain is depicted in Figure 4. Strong ECG artifacts were introduced and QRS-like spikes were observed in the corrupted EEG signal. After denoising with RLS algorithm, these spikes were effectively suppressed (Figure 4F). However, FastICA and Infomax failed to remove the cardiac artifacts (Figure 4D, 4E).

Figure 5 shows the comparison of INPS and MSE values among three methods at different SNR levels in simulated data after removing ECG artifacts. Taking all SNR levels in to consideration, INPS for the RLS method (19.75(18.37, 20.95) dB) was significantly higher than that of FastICA (4.35(3.35,5.41) dB) and Infomax (5.76(4.60,6.88) dB) ($P<0.05$). MSE for the RLS method (0.20(0.08,0.53) μV^2) was remarkably lower than that of FastICA (5.59(2.35, 19.79) μV^2) and Infomax (3.21(1.01, 10.69) μV^2) ($P<0.05$). At each SNR level, INPS of RLS method was notably higher

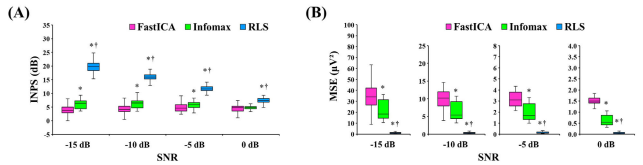

FIGURE 5. The comparison of INPS and MSE among three methods at different SNRs in simulated data (A) INPS (B) MSE. INPS, improvement of normalized power spectrum. MSE, mean square error. SNR, signal to noise ratio. ICA, independent component analysis. Infomax, information maximization. RLS, recursive least squares. * P<0.05 compared with FastICA; †P<0.05 compared with Infomax.

than that of other two methods (P<0.05) and MSE of RLS method was dramatically lower than that of other two methods (P<0.05). In addition, INPS of Infomax method was notoriously higher than that of FastICA approach (P<0.05) and MSE of Infomax method was relatively lower than that of FastICA approach (P<0.05).

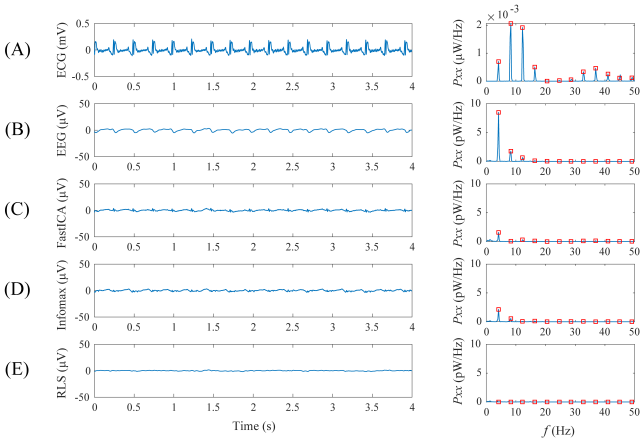

FIGURE 6. An example of isoelectric EEG from animal experimental data before and after removing ECG artifacts in time and frequency domain. (A) ECG (B) real EEG (C) FastICA (D) Infomax (E) RLS. The power spectral density (P_{xx}) is calculated using the Welch method and 4-s rectangular window. Red square markers shown in the frequency domain represent ECG harmonics. ICA, independent component analysis. Infomax, information maximization. RLS, recursive least squares.

B. REMOVING ECG ARTIFACTS FROM ANIMAL EXPERIMENTAL DATA

An example of isoelectric EEG from animal experimental data before and after removing ECG artifacts in both time and frequency domain is illustrated in Figure 6. Isoelectric EEG was seriously influenced by cardiac interference with quasi-periodic like artifacts (Figure 6B). After signal denoising, FastICA and Infomax methods both failed to remove ECG artifacts (Figure 6C, 6D). It can be observed a clearly isoelectric EEG after rejecting ECG artifacts using RLS method (Figure 6E).

An example of burst suppression EEG from animal experimental data before and after removing ECG artifacts in time and frequency domain is illustrated in Figure 7. After signal denoising, FastICA and Infomax methods both failed to remove ECG artifacts from the artifact-contaminated burst suppression EEG signals (Figure 7C, 7D). The ECG artifacts were removed from the artifact-contaminated EEG signals (Figure 7E).

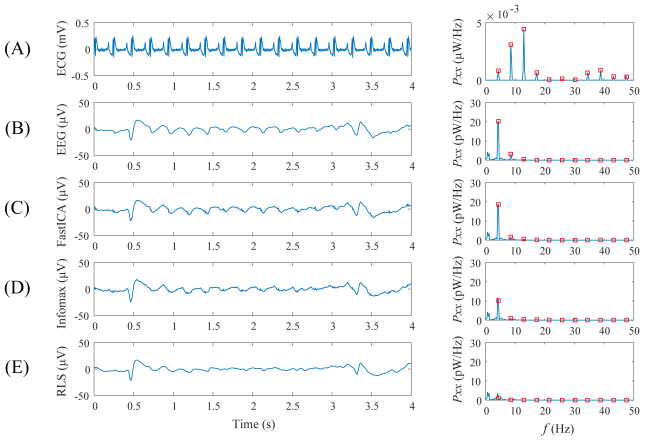

FIGURE 7. An example of burst suppression EEG from animal experimental data before and after removing ECG artifacts in time and frequency domain. (A) ECG (B) real EEG (C) FastICA (D) Infomax (E) RLS. The power spectral density (P_{xx}) is calculated using the Welch method and 4-s rectangular window. Red square markers shown in the frequency domain represent ECG harmonics. ICA, independent component analysis. Infomax, information maximization. RLS, recursive least squares.

An example of continuous background EEG from animal experimental data before and after removing ECG artifacts in time and frequency domain is illustrated in Figure 8. After denoising, FastICA failed to remove ECG artifacts from the continuous background EEG signals (Figure 8C). The ECG artifacts were removed from the artifact-contaminated EEG signals by RLS and Infomax methods (Figure 8D, 8E).

Figure 9 (A) shows INPS in animal experimental data after removing ECG artifacts using three methods. Taking all EEG rhythms into consideration, INPS for the RLS method (1.76(0.42,9.40) dB) was significantly higher than that of FastICA (0.02(0.00,0.14) dB) and Infomax (0.57(0.08,2.45) dB) (P<0.05). After denoising, in isoelectric EEG, INPS for the RLS method (12.97(7.63,16.68) dB), was remarkably higher than that of Infomax (2.70(1.02,5.03) dB) and FastICA (0.06(0.01,0.22) dB) (P<0.05). In burst suppression EEG, INPS for the RLS method (1.20(0.35,3.36) dB) was notably higher than that of Infomax (0.30(0.03,1.49) dB) and FastICA (0.00(0.00,0.07) dB) (P<0.05). In continuous background EEG, INPS for the RLS method (0.39(0.18,0.76) dB) was considerably higher than that of Infomax (0.08(−0.06,0.28) dB) and FastICA (0.04(0.00,0.20) dB) (P<0.05).

Figure 9 (B) shows IQ of the EEG signal before and after removing ECG artifacts with FastICA, Infomax and RLS. Taking all EEG rhythms into consideration, IQ for the RLS method (0.331(0.021,0.584)) was significantly lower than that of raw EEG (0.350(0.070,0.586)), FastICA (0.350(0.069,0.581)) and Infomax (0.341(0.050,0.585)) (P<0.05). The IQ of raw EEG signals was 0.049(0.011,0.094) in isoelectric EEG, 0.403(0.273,0.515) in burst suppression

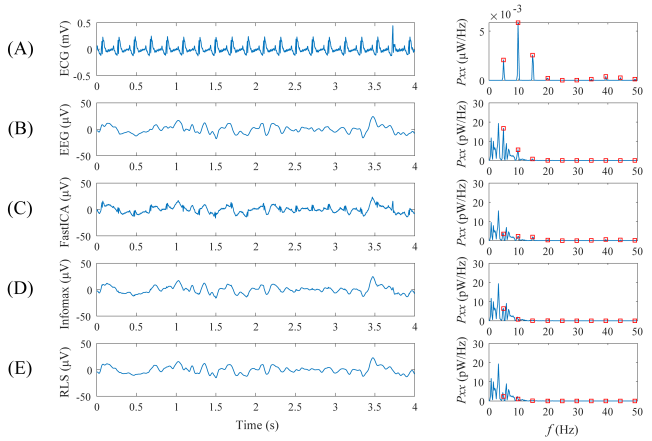

FIGURE 8. An example of continuous background EEG from animal experimental data before and after removing ECG artifacts in time and frequency domain. (A) ECG (B) real EEG (C) FastICA (D) Infomax (E) RLS. The power spectral density (P_{xx}) is calculated using the Welch method and 4-s rectangular window. Red square markers shown in the frequency domain represent ECG harmonics. ICA, independent component analysis. Infomax, information maximization. RLS, recursive least squares.

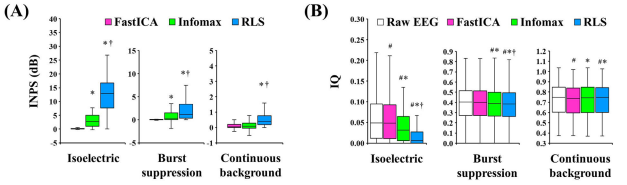

FIGURE 9. INPS and IQ of FastICA, Infomax and RLS methods in animal experimental data after ECG artifacts suppression. (A) INPS (B) IQ. INPS, improvement of normalized power spectrum. IQ, information quantity. ICA, independent component analysis. Infomax, information maximization. RLS, recursive least squares. #: P<0.05 compared with raw EEG; *: P<0.05 compared with FastICA; †: P<0.05 compared with Infomax method.

EEG, 0.747(0.604,0.848) in continuous background EEG. After removing ECG artifacts, IQ values were considerably reduced when different methods were applied. After denoising, in isoelectric EEG, IQ for the RLS method (0.006(0.000,0.027)) was notably lower than that of Infomax (0.031(0.006,0.064)) and FastICA (0.048(0.011,0.092)) (P<0.05). In burst suppression EEG, IQ for the RLS method (0.384(0.263,0.493)) was dramatically lower than that of Infomax (0.389(0.266,0.500)) and FastICA (0.402(0.272, 0.513)) (P<0.05). In continuous background EEG IQ for the RLS method (0.746(0.601,0.843)) relatively higher than that of FastICA (0.737(0.597,0.839)) (P<0.05) and was lower than that of Infomax (0.745(0.600,0.848)) but not reach the significant level.

IV. DISCUSSION

This study introduces a new ECG artifacts cancellation method based on an artifact model that needs the instantaneous frequency of the cardiac cycle as additional information, and only a single-channel EEG and ECG were used. Using the frequency of the successive R peaks as the fundamental frequency, a Fourier series representation of the ECG artifacts was proposed with time-varying coefficients to reflect changes in waveform from R peak to R peak. A RLS filter adaptively estimates the coefficients without any parameters to be determined. Simulated and animal experimental data revealed that the RLS notch filter can not only remove the ECG artifacts effectively, but also preserve the majority of EEG information.

The improved performance of the RLS method may result from the following two aspects. On the one hand, the only information used by the RLS adaptive scheme is the time series of R peaks. Using an ECG channel as the reference signal, previous study introduced an adaptive filtering artifact method to cancel ECG artifacts from sleep EEG [30]. Strobach et al revealed that this adaptive approach may be not applicable when the ECG signal and the real cardiac interference show remarkably different waveforms [12]. To further improve the performance of adaptive filter, they developed a two-pass adaptive filtering algorithm where an artificial reference was first generated by ensemble averaging, to be more related to the real interference than the ECG [12]. Nevertheless, as long as there are reference signals used for the adaptive filter, ECG artifacts may be overestimated and some useful EEG information may be lost after filtering since there is a cross-interference between the reference signal and EEG [9]. In the proposed RLS method, the artifacts model was generated using instantaneous harmonic frequency of each cardiac cycle and then was subtracted by corrupted EEG signal. This process is robust for ECG artifacts rejection because only ECG harmonic-related components can be removed and underlying EEG information was preserved with little information loss. As a consequence, INPS of the RLS method was improved in both simulated and animal experimental data.

On the other hand, rapid initial convergence and narrow bandwidth may partly contribute to the improved performance of the RLS method. RLS scheme is an algorithm commonly used in adaptive filtering and it exhibits extremely fast convergence due its second-order nature [9]. Previous study has shown that the LMS adaptive notch filter can be used to remove the baseline wandering in ECGs [31]. The stepsize of LMS method not only determines how fast and how well the algorithm converges to the optimum filter coefficients, but also determines filter bandwidth [21]. If the stepsize is too large, the LMS algorithm will not converge, and the bandwidth will adaptively increase, causing the energy of other EEG bands damaged. Otherwise, the LMS algorithm converges slowly and the bandwidth is too narrow, making it insufficient to cancel interference. Thus, it is hard to choose an appropriate stepsize to get the best performance of the LMS method. Consistent with previous study [32], our results showed that the proposed RLS method has a narrow bandwidth and did not damage underlying EEG rhythm with low MSE values (Figure 3). In addition, the RLS method is not required to determine any parameters when denoising ECG artifacts since RLS notch filter does not largely depend on the change of forgetting factor (Figure 3).

ICA may not be an appropriate approach for cardiac interference cancellation when only an EEG channel and an ECG reference channel are available. This method assumes that the subcomponents are non-Gaussian signals, but sometimes EEG was presented like a Gaussian signal (Figure 8). Another possible explanation is that ICA seems to be incapable of separating the real cardiac interference whose waveforms are remarkably different from ECG [11]. Moreover, directly set ECG artifacts-related components to zero may damage the underlying EEG information when using the ICA method, especially in only single channel EEG and ECG situation since the available information is too little [8]. Therefore, in our study, ICA method failed to eliminate ECG interference (Figure 6, 7, 8). Furthermore, artifactual components should be manually detected by visual inspection when using the ICA method, which is time consuming and subjective [6], [33]–[36].

Blind deconvolution can remove cardiac interference to some extent, but it also introduces spike-like artifacts in the isoelectric and burst suppression situations (Figure 5, 6) possibly because different waveforms between cardiac artifacts and the ECG signal may sometimes decrease the performance of the Infomax processes [11]. In addition, two parameters, stepsize and filter length, of this method are required to adjust, and the convergence speed of this algorithm is sometimes relatively low [37].

The proposed RLS method achieved obvious performance enhancement in terms of INPS and IQ after cardiac interference removal in animal experimental data. In the first place, significantly improved INPS values were observed in all EEG rhythms, which demonstrated that ECG artifacts were effectively removed from the original EEG signals. But in continuous background EEG, there was little improvement in terms of INPS for RLS method when compared with that Infomax method, and it may be largely due to that the energy of ECG artifacts is extremely smaller than the energy of continuous background EEG and so low INPS after removing artifacts was observed. In the second place, significantly lower IQ was observed after removing ECG artifacts, which demonstrated that the ECG artifacts contribute to the overestimated brain activity. IQ has been extensively used to measure the brain activity and predict outcome after ischemic brain injury [38], [39]. Higher IQ corresponds to greater randomness measured by the entropy of the EEG rhythm; as such, a healthier brain exhibits higher entropy and injured brain lower entropy. Thus, patients with higher IQ due to ECG artifacts may provide unreliable information for their doctors and would make them miss the optimal treatment timing. In this study, the proposed method can effectively reject ECG artifacts from EEG signals and preserve the majority of EEG information with little loss, which may provide credible information of brain activity.

Our study has several limitations. Firstly, this method can be used to remove cardiac harmonics, but it did not test on EEG data corrupted by other artifacts. Secondly, the effect of the number of harmonics on the performance of RLS method was not investigated in this study. We simply set $N = 25$ because the heart rate of rats is usually higher than 300 beats per minute (5 Hz) and the frequency of the 25th harmonics is larger than 125Hz which exceeds the meaningful bands of EEG. Lastly, the study was performed in animals. Electrophysiological differences between human and small animals are remarkably, especially in ECG. In the human, the fundamental frequency of the heart rate is around 1.2 Hz and the frequencies of its harmonics overlap with all brain rhythms (delta, theta, alpha, beta, gamma). Thus, this method should be more cautiously applied into clinical circumstance due to the higher overlaps between cardiac interference and brain activity.

V. CONCLUSION

A RLS notch filter was developed to remove ECG artifacts from EEG and it needs only the instantaneous frequency of the cardiac cycle as additional information. This method can be successfully applied in suppression of the ECG interference without distortion of background EEG activity, which may provide a viable approach for removal of other artifacts from EEG, like electromyography and electrooculography artifacts.

AUTHOR CONTRIBUTION

(Jianjie Wang and Chenxi Dai are co-first authors.)

REFERENCES

[1] W. O. Tatum, A. Husain, and S. Bembadis, *Handbook of EEG Interpretation*. New York, NY, USA: Demos Medical, 2007.

[2] M. Waser and H. Garn, "Removing cardiac interference from the electroencephalogram using a modified Pan-Tompkins algorithm and linear regression," in *Proc. 35th Annu. Int. Conf. IEEE Eng. Med. Biol. Soc. (EMBC)*, Jul. 2013, pp. 2028–2031.

[3] E. Harmon-Jones, *Cognitive Dissonance Theory*. London, U.K.: Academic, 2012.

[4] M. R. Nuwer, "Quantitative EEG: I. Techniques and problems of frequency analysis and topographic mapping," *J. Clin. Neurophysiol.*, vol. 5, no. 1, pp. 1–44, 1988.

[5] M. R. Nuwer, "Quantitative EEG: II. Frequency analysis and topographic mapping in clinical settings," *J. Clin. Neurophysiol.*, vol. 5, no. 1, pp. 45–86, 1988.

[6] M. B. Hamaneh, N. Chitravas, K. Kaiboriboon, S. D. Lhatoo, and K. A. Loparo, "Automated removal of EKG artifact from EEG data using independent component analysis and continuous wavelet transformation," *IEEE Trans. Biomed. Eng.*, vol. 61, no. 6, pp. 1634–1641, Jun. 2014.

[7] J. Sijbers, J. Van Audekerke, M. Verhoye, A. Van der Linden, and D. Van Dyck, "Reduction of ECG and gradient related artifacts in simultaneously recorded human EEG/MRI data," *Magn. Reson. Imag.*, vol. 18, no. 7, pp. 881–886, 2000.

[8] S. Tong, A. Bezerianos, J. Paul, Y. Zhu, and N. Thakor, "Removal of ECG interference from the EEG recordings in small animals using independent component analysis," *J. Neurosci. Methods*, vol. 108, no. 1, pp. 11–17, 2001.

[9] K. T. Sweeney, T. E. Ward, and S. F. McLoone, "Artifact removal in physiological signals—Practices and possibilities," *IEEE Trans. Inf. Technol. Biomed.*, vol. 16, no. 3, pp. 488–500, May 2012.

[10] J. Iriarte, E. Urrestarazu, M. Valencia, M. Alegre, A. Malanda, C. Viteri, and J. Artieda, "Independent component analysis as a tool to eliminate artifacts in EEG: A quantitative study," *J. Clin. Neurophysiol.*, vol. 20, no. 4, pp. 249–257, 2003.

[11] S. Devuyst, T. Dutoit, P. Stenuit, M. Kerkhofs, and E. Stanus, "Removal of ECG artifacts from EEG using a modified independent component analysis approach," in *Proc. 30th Annu. Int. Conf. IEEE Eng. Med. Biol. Soc.*, vol. 30, no. 1, Aug. 2008, pp. 5204–5207.

[12] P. Strobach, K. Abraham-Fuchs, and W. Harer, "Event-synchronous cancellation of the heart interference in biomedical signals," *IEEE Trans. Biomed. Eng.*, vol. 41, no. 4, pp. 343–350, Apr. 1994.
[13] S. V. Narasimhan and D. N. Dutt, "Application of LMS adaptive predictive filtering for muscle artifact (noise) cancellation from EEG signals," *Comput. Elect. Eng.*, vol. 22, no. 1, pp. 13–30, 1996.
[14] A. G. Correa, E. Laciar, H. D. Patiño, and M. E. Valentinuzzi, "Artifact removal from EEG signals using adaptive filters in cascade," *J. Phys., Conf. Ser.*, vol. 90, no. 1, 2007, Art. no. 012081.
[15] P. S. Kumar, R. Arumuganathan, K. Sivakumar, and C. Vimal, "Removal of artifacts from EEG signals using adaptive filter through wavelet transform," in *Proc. 9th Int. Conf. Signal Process. (ICSP)*, Oct. 2008, pp. 2138–2141.
[16] B. Chen, G. Chen, C. Dai, P. Wang, L. Zhang, Y. Huang, and Y. Li, "Comparison of quantitative characteristics of early post-resuscitation EEG between asphyxial and ventricular fibrillation cardiac arrest in rats," *Neurocritical Care*, vol. 28, no. 2, pp. 247–256, 2018.
[17] B. Chen, F.-Q. Song, L.-L. Sun, L.-Y. Lei, W.-N. Gan, M.-H. Chen, and Y. Li, "Improved early postresuscitation EEG activity for animals treated with hypothermia predicted 96 hr neurological outcome and survival in a rat model of cardiac arrest," *BioMed Res. Int.*, vol. 2013, Oct. 2013, Art. no. 312137.
[18] M. He, Y. Nian, and Y. Gong, "Novel signal processing method for vital sign monitoring using FMCW radar," *Biomed. Signal Process. Control*, vol. 33, pp. 335–345, Mar. 2017.
[19] A. Stefanovska, H. Haken, P. V. E. McClintock, M. Hožič, F. Bajrović, and S. Ribarič, "Reversible transitions between synchronization states of the cardiorespiratory system," *Phys. Rev. Lett.*, vol. 85, no. 22, pp. 4831–4834, 2000.
[20] J. Pan and W. J. Tompkins, "A real-time QRS detection algorithm," *IEEE Trans. Biomed. Eng.*, vol. BME-32, no. 3, pp. 230–236, Mar. 1985.
[21] Y. Xiao and Y. Tadokoro, "LMS-based notch filter for the estimation of sinusoidal signals in noise," *Signal Process.*, vol. 46, no. 2, pp. 223–231, 1995.
[22] E. Eleftheriou and D. Falconer, "Tracking properties and steady-state performance of RLS adaptive filter algorithms," *IEEE Trans. Acoust., Speech, Signal Process.*, vol. ASSP-34, no. 5, pp. 1097–1110, Oct. 1986.
[23] S. Rogers, "Adaptive filter theory," *Control Eng. Pract.*, vol. 4, no. 11, pp. 1629–1630, 1996.
[24] J. Glover, "Adaptive noise canceling applied to sinusoidal interferences," *IEEE Trans. Acoust., Speech, Signal Process.*, vol. ASSP-25, no. 6, pp. 484–491, Dec. 1977.
[25] B. Widrow, J. R. Glover, J. M. McCool, J. Kaunitz, C. S. Williams, R. H. Hearn, J. R. Zeidler, Jr. E. Dong, and R. C. Goodlin, "Adaptive noise cancelling: Principles and applications," *Proc. IEEE*, vol. 63, no. 12, pp. 1692–1716, Dec. 1975.
[26] V. Van Vaerenberg, M. Lazaro-Gredilla, and I. Santamaria, "Kernel recursive least-squares tracker for time-varying regression," *IEEE Trans. Neural Netw. Learn. Syst.*, vol. 23, no. 8, pp. 1313–1326, Aug. 2012.
[27] S. Devuyst, T. Dutoit, P. Stenuit, M. Kerkhofs, and E. Stanus, "Cancelling ECG artifacts in EEG using a modified independent component analysis approach," *Eurasip J. Adv. Signal Process.*, vol. 2008, Dec. 2008, Art. no. 747325.
[28] M. Rundgren, I. Rosén, and H. Friberg, "Amplitude-integrated EEG (aEEG) predicts outcome after cardiac arrest and induced hypothermia," *Intensive Care Med.*, vol. 32, no. 6, pp. 836–842, 2006.
[29] H.-C. Shin, S. Tong, S. Yamashita, X. Jia, G. Geocadin, and V. Thakor, "Quantitative EEG and effect of hypothermia on brain recovery after cardiac arrest," *IEEE Trans. Biomed. Eng.*, vol. 53, no. 6, pp. 1016–1023, Jun. 2006.
[30] Z. Sahul, J. Black, B. Widrow, and C. Guilleminault, "EKG artifact cancellation from sleep EEG using adaptive filtering," *Sleep Res. A*, vol. 24A, p. 486, Jan. 1995.
[31] N. V. Thakor and Y.-S. Zhu, "Applications of adaptive filtering to ECG analysis: Noise cancellation and arrhythmia detection," *IEEE Trans. Biomed. Eng.*, vol. 38, no. 8, pp. 785–794, Aug. 1991.
[32] W. K. Ma, Y. T. Zhang, and F. S. Yang, "A fast recursive-least-squares adaptive notch filter and its applications to biomedical signals," *Med. Biol. Eng. Comput.*, vol. 37, no. 1, pp. 99–103, 1999.
[33] W. Zhou and J. Gotman, "Removal of EMG and ECG artifacts from EEG based on wavelet transform and ICA," in *Proc. 26th Annu. Int. Conf. IEEE Eng. Med. Biol. Soc. (EMBS)*, vol. 1, Sep. 2004, pp. 392–395.
[34] S. Romero, M. A. Mananas, S. Clos, S. Gimenez, and M. J. Barbanoj, "Reduction of EEG artifacts by ICA in different sleep stages," in *Proc. EEE Eng. Med. Biol. Soc.*, Sep. 2003, pp. 2675–2678.
[35] N. Ille, P. Berg, and M. Scherg, "Artifact correction of the ongoing EEG using spatial filters based on artifact and brain signal topographies," *J. Clin. Neurophysiol.*, vol. 19, no. 2, pp. 113–124, 2002.
[36] J.-P. Lanquart, M. Dumont, and P. Linkowski, "QRS artifact elimination on full night sleep EEG," *Med. Eng. Phys.*, vol. 28, no. 2, pp. 156–165, 2006.
[37] J. Chua, G. Wang, and B. W. Kleijn, "Convolutive blind source separation with low latency," in *Proc. IEEE Int. Workshop Acoustic Signal Enhancement*, Sep. 2016, pp. 1–5.
[38] X. Jia, M. A. Koenig, H.-C. Shin, G. Zhen, S. Yamashita, N. V. Thakor, and R. G. Geocadin, "Quantitative EEG and neurological recovery with therapeutic hypothermia after asphyxial cardiac arrest in rats," *Brain Res.*, vol. 1111, no. 1, pp. 166–175, 2006.
[39] Q. Wang, P. Miao, H. R. Modi, S. Garikapati, R. C. Koehler, and N. V. Thakor, "Therapeutic hypothermia promotes cerebral blood flow recovery and brain homeostasis after resuscitation from cardiac arrest in a rat model," *J. Cerebral Blood Flow Metabolism*, vol. 39, no. 10, pp. 1961–1973, 2019.